A model relating transpiration for Japanese cedar and cypress plantations with stand structure

AUTHOR(S):

Komatsu, Hikaru; Shinohara, Yoshinori; Kumagai, Tomo'omi; Kume, Tomonori; Tsuruta, Kenji; Xiang, Yang; Ichihashi, Ryuji; ... Ogura, Akira; Saito, Takami; Otsuki, Kyoichi

CITATION:

Komatsu, Hikaru ...[et al]. A model relating transpiration for Japanese cedar and cypress plantations with stand structure. Forest Ecology and Management 2014, 334: 301-312

ISSUE DATE:

2014-12-15

URL:

http://hdl.handle.net/2433/191207

1 Title

2 A model relating transpiration for Japanese cedar and cypress plantations with stand
3 structure

4

5 The name and the affiliation of the authors

6 Hikaru Komatsu[1,2 *], Yoshinori Shinohara[3], Tomo'omi Kumagai[4], Tomonori Kume[5],
7 Kenji Tsuruta[2], Yang Xiang[6], Ryuji Ichihashi[6], Makiko Tateishi[6], Takanori Shimizu[7],
8 Yoshiyuki Miyazawa[8], Mari Nogata[6], Sophie Laplace[5], Tseng Han[5], Chen-Wei Chiu[6],
9 Akira Ogura[9], Takami Saito[4], Kyoichi Otsuki[6]

10

11 [1] The Hakubi Center for Advanced Research, Kyoto University, Kyoto 606–8302, Japan

12 [2] Graduate School of Agriculture, Kyoto University, Kyoto 606-8502, Japan

13 [3] Faculty of Agriculture, Kyushu University, Fukuoka 812-8581, Japan

14 [4] Hydrospheric Atmospheric Research Center, Nagoya University, Chikusa-ku, Nagoya
15 464-8601, Japan

16 [5] School of Forestry and Resource Conservation, National Taiwan University, Taipei 106,
17 Taiwan

18 [6] Kasuya Research Forest, Kyushu University, Fukuoka 811-2415, Japan

19 [7] Forestry and Forest Products Research Institute, Matsunosato, Tsukuba, Ibaraki 305-
20 8687, Japan

[8] Research Institute for East Asia Environments, Kyushu University, Motooka, Fukuoka 811-0395, Japan

[9] Ishikawa-ken Forest Experimental Station, Ishikawa 920-2114, Japan

* Corresponding author

Full address, E-mail, telephone, and fax numbers:

Hikaru Komatsu, The Hakubi Center for Advanced Research, Kyoto University, Kyoto 606–8302, Japan

Tel/Fax: +81–75–753–5100/5310

E-mail: kmthkr@gmail.com

Abstract

Previous studies have revealed that changes in forest structure due to management (e.g., thinning, aging, and clearcutting) could affect the forest water balance. However, there are unexplained variability in changes in the annual water balance with changing structure among different sites. This is the case even when analyzing data for specific species/regions. For a more advanced and process-based understanding of changes in the water balance with changing forest structure, we examined transpiration (E) observed using the sap-flux method for 14 Japanese cedar and cypress plantations with various structure (e.g., stem density and diameter) in Japan and surrounding areas and developed a model relating E with structural parameters. We expressed E using the simplified Penman–Monteith equation and modeled canopy conductance (G_c) as a product of reference G_c (G_{cref}) when vapor pressure deficit is 1.0 kPa and functions expressing the responses of G_c to meteorological factors. We determined G_{cref} and parameters of the functions for the sites separately. E observed for the 14 sites was not reproduced well by the model when using mean values of G_{cref} and the parameters among the sites. However, E observed for the sites was reproduced well when using G_{cref} determined for each site and mean values of the parameters of the functions among the sites, similar to the case when using G_{cref} and the parameters of the functions determined for each site. These results suggest that considering variations in G_{cref} among the sites was important to reproduce variations in E, but considering variations in the parameters of the functions

52 was not. Our analysis revealed that G_{cref} linearly related with the sapwood area on a stand
53 scale (A) and that A linearly related with stem density (N) and powers of the mean stem
54 diameter (d_m). Thus, we proposed a model relating E with A (or N and d_m), where G_{cref}
55 was calculated from A (or N and d_m) and the parameters of the functions were assumed to
56 be the mean values among the sites. This model estimates changes in E with changing
57 structure from commonly available data (N and d_m), and therefore helps improve our
58 understanding of the underlying processes of the changes in the water balance for
59 Japanese cedar and cypress plantations.
60
61 Key words: canopy conductance; forest structure; model; sapwood area; simplified
62 Penman–Monteith equation; transpiration
63

1. Introduction

Changes in forest structure due to management (e.g., planting, growth, thinning, aging, and clearcutting) can affect the forest water balance. Numerous studies (Scott and Lesch, 1997; Cornish and Vertessy, 2001) have examined changes in the annual water balance with changing forest structure on the basis of catchment water balance data. Summarizing data derived from such studies and analyzing them using linear regression, researchers have identified several important parameters (e.g., the ratio of the cutting area to the total catchment area, annual rainfall, and leaf phenology) determining changes in annual runoff with changing structure (Bosch and Hewlett, 1982; Brown et al., 2005; Komatsu et al., 2011). However, there remains unexplained variability in changes in the annual water balance (Bosch and Hewlett, 1982; Brown et al., 2005). This is the case even for data for a single species within a specific region, although the variability is less pronounced (Adams and Fowler, 2006; Komatsu et al., 2011). This suggests the limitation of analyzing catchment water balance data simply using linear regression without considering underlying processes (e.g., canopy transpiration and interception evaporation). For a more advanced understanding of changes in the annual water balance with changing structure, examining relationships of canopy transpiration and interception for given species with various structure (e.g., stem density and diameter) would be useful (Komatsu et al., 2007d). Variations in stem density and diameter relate with the sapwood area on a stand scale and leaf area index, which could in turn relate with canopy

84 transpiration (Granier et al., 2000a; Ewers et al., 2011). Focusing on specific species
85 would be useful in reducing factors to be considered, because there are factors (e.g., the
86 clumpling factor and stem conductivity) that could differ among different species and
87 affect canopy transpiration (Baldocchi and Meyers, 1998; Zwieniecki and Holbrook,
88 1998; Bréda, 2003).

89 Japanese cedar (*Cryptomeria japonica*) and cypress (*Chamaeryparis obtusa*) are
90 major plantation species in Japan and surrounding areas such as China and Taiwan (Japan
91 Forestry Agency, 2014). Examining the water balance of these plantations is highly
92 important from a practical viewpoint. Forest management (e.g., thinning) has been
93 performed to increase water resources in Japan, although its effectiveness has not been
94 assessed sufficiently (Komatsu et al., 2010). Summarizing data for interception
95 evaporation of Japanese cedar and cypress plantations (Hattori et al., 1982; Tanaka et al.,
96 2005), Komatsu et al. (2007a) found a relationship between stem density and interception
97 evaporation and then developed a model relating interception evaporation with stem
98 density. However, there have been few studies examining the relationship between forest
99 structure and canopy transpiration (E) for Japanese cedar and cypress plantations.

100 To assess changes in the water balance of Japanese cedar and cypress plantations
101 with changing forest structure, we developed a model relating E for Japanese cedar and
102 cypress plantations with meteorological and structural variables. The model formulates E
103 using the simplified Penman–Monteith equation (McNaughton and Black, 1973; Jarvis

and McNaughton, 1986). Canopy conductance (G_c) in the equation was written as a series of functions expressing responses of G_c to meteorological factors (Jarvis, 1976; Lohammer et al., 1980). This study comprises three steps. First, we calculated G_c using E data derived employing the sap-flux method for 14 sites and the inverted form of the simplified Penman–Monteith equation to determine parameters of the model for the sites separately. Second, we assessed the importance of each parameter in determining E on the basis of sensitivity analysis. Third, we examined the relationship of the important parameters with structural parameters. Here, we tried to relate the structural parameters with commonly available data such as stem density and diameter for wide use of the model.

Models estimating E are roughly classified into two groups. One uses many empirical parameters for modeling stomatal/canopy conductance to avoid considering internal hydraulics and keep the model structure simple (Granier et al., 2000a; Komatsu, 2004), while the other considers internal hydraulics (Domec et al., 2012; McDowell et al., 2013). Our model belongs to the former group. Most models of the former group focus on reproducing E for a specific site (Cienciala et al., 1994a,b; Granier and Bréda, 1996). Several models (Granier et al., 2000a; Komatsu, 2004) are applicable to various sites, similar to our model. Our model differs from these models in that our model focuses on two species, which suggests higher predictability of the model when applied to the species. Furthermore, our model differs from the models in that our model would be tested against

124 *E* data recorded not only during growing seasons but during winter, suggesting higher
125 reliability of the model to predict *E* on a long time scale (e.g., one year).
126
127 2. Theory
128 The model, using the simplified Penman–Monteith equation (McNaughton and
129 Black, 1973; Jarvis and McNaughton, 1986), expresses *E* as
130 $$E = \frac{\rho C_p G_c D}{\gamma \lambda}, \quad (1)$$
131 where ρ is the air density, C_p is the specific heat of air, G_c is canopy conductance, D is
132 the vapor pressure deficit, γ is the psychrometric constant, and λ is the latent heat of water
133 vaporization. This equation is derived from the Penman–Monteith equation under the
134 assumption of complete coupling between the canopy and atmosphere.
135 G_c is formulated as a product of the reference value of G_c when D is 1.0 kPa
136 (G_{cref}, Oren et al., 1999) and functions expressing responses of G_c to meteorological
137 factors (Jarvis, 1976; Lohammer et al., 1980):
138 $$G_c = G_{cref} \cdot f(D) \cdot g(R) \cdot h(T), \quad (2)$$
139 where $f(D)$, $g(R)$, and $h(T)$ are functions expressing the responses of G_c to mean daytime
140 D, solar radiation (R), and air temperature (T), respectively. $f(D)$, $g(R)$, and $h(T)$ are
141 respectively modeled as (Oren et al., 1999; Granier et al., 2000b)
142 $$f(D) = 1.00 - \beta \cdot ln(D), \quad (3)$$
143 $$g(R) = \min\left\{\left(\frac{R}{600}\right)^{\delta}, 1.00\right\}, \quad (4)$$

$$h(T) = \begin{cases} 1.00 & (T \geq \epsilon) \\ \frac{T-\zeta}{\epsilon-\zeta} & (\zeta < T < \epsilon) \\ 0.00 & (T \leq \zeta) \end{cases}, \qquad (5)$$

where β, δ, ε, and ζ are parameters. The model does not consider the effect of the soil water deficit on G_c. Most previous studies, making continuous measurements of E (or its substitutes) for forests in Japan including Japanese cedar and cypress plantations (Komatsu et al., 2006; Kosugi et al., 2007; Kumagai et al., 2007), did not report a clear reduction in G_c or E with a soil water deficit, although there were a few exceptions (Tanaka et al., 2002; Komatsu et al., 2007c).

We hypothesized that considering the variation in G_{cref} among sites would be important but considering variations in β, δ, ε, and ζ among sites would not be in reproducing E for the sites. Our hypothesis was based on results of previous studies. G_{cref} linearly relates with E in the simplified Penman–Monteith equation. G_{cref} values reported previously (Granier et al., 2000a; Komatsu et al., 2012, 2013) often differ greatly among different forest sites comprising the same species, implying that considering the variation in G_{cref} among the sites is important in estimating E. Oren et al. (1999) and succeeding studies (Addington et al., 2004; Ewers et al., 2008) noted a fairly conservative β among different sites. Thus, assuming β as constant among sites might not introduce large errors in E estimates. Komatsu et al. (2006) analyzed sap flux data on an hourly time scale for a Japanese cedar plantation and pointed out that the control of G_c by R was important only

early in the morning and late afternoon, when E is small. This implies that assuming δ as constant among sites would not introduce large errors in estimating E on a daily time scale. ε and ζ affect E during winter, which accounts for a small portion of annual E for Japanese cedar and cypress plantations (Suzuki, 1980; Kumagai et al., 2014). Thus, assuming ε and ζ as constant among sites might not introduce large errors in estimating E on a longer time scale, such as one year.

We further hypothesized that G_{cref} would relate with the sapwood area on a stand scale (A) for the following reasons. Kumagai et al. (2007) examined E for two cedar forest sites located nearby but having different A. The relative difference in E between the sites was comparable to that in A. Komatsu et al. (2013) compared E values for a cedar forest during two successive growing seasons just before and after thinning. The ratio of E after thinning to that before thinning approximated the ratio of A after thinning to that before thinning. The results of Kumagai et al. (2007) and Komatsu et al. (2013) suggest a correlation between A and G_{cref}. Previous studies (Macfarlane et al., 2010; Ewers et al., 2011) reported relationships between A and E for forests comprising other species. These results also suggest that our hypothesis is reasonable. The relationship between A and G_{cref} would allow the estimation of G_{cref} with the input of A, and then the estimation of E by assuming typical values of β, δ, ε, and ζ and using the simplified Penman–Monteith equation.

3. Data used

We used E data recorded for nine Japanese cedar and five Japanese cypress plantations (Table 1). Twelve of the 14 sites were located in western Japan, but the IK and XT sites were located in eastern Japan and in Taiwan, respectively. Structural parameters differed among the sites. Stem density (N) ranged between 600 and 1575 stems ha^{-1} for cedar and between 350 and 2100 stems ha^{-1} for cypress. The mean diameter at breast height (d_m) ranged between 13.5 and 48.4 cm. The leaf area index (L), estimated using optical methods (see the footnote #2 of Table 1), ranged between 0.8 and 5.9 m^2 m^{-2} for cedar and between 0.8 and 4.8 m^2 m^{-2} for cypress. Note that L for Japanese cedar and cypress forests estimated using optical methods is generally lower than that estimated using destructive leaf sampling and/or allometry equations (Hasegawa et al., 2013; Tsuruta et al., 2014). The sapwood area at a stand scale (A) ranged between 14.1 and 46.0 m^2 ha^{-1} for cedar and between 8.8 and 20.4 m^2 m^{-2} for cypress. A was determined by measurements of sapwood thickness using core sampling and assuming the stem cross-section was circular. A complete description of the measurements was provided by Kumagai et al. (2007) and Kume et al. (2010).

E values for all sites were measured employing the sap-flux method and Granier sensors (Granier, 1987). A detailed description of the measurements is available in the papers cited in Table 1. Employing the method, E was estimated as (Kumagai et al., 2007; Kume et al., 2010)

202 $$E = \frac{\sum_{i=1}^{n} F_i \cdot a_i}{S}, \quad (6)$$

203 where F is the sap flux for an individual tree averaged over its sapwood area, a is the tree
204 sapwood area, n is the number of trees in the plot, and S is the ground area. For a tree
205 whose sapwood thickness was much greater than the sensor length (i.e., 2.0 cm), two or
206 three sensors were installed radially to cover the sapwood area (Kumagai et al., 2007). F
207 was calculated as the weighted average of sap flux for the sensors. Azimuthal variations
208 of sap flux were also considered for some sites (Shinohara et al., 2013a).

209

210 4. Methods of analysis

211 4.1. Determination of parameters

212 We calculated canopy conductance (G_c) from E estimated using the sap-flux
213 method and meteorological factors for each site using the inverted form of the simplified
214 Penman–Monteith equation:

215 $$G_c = \frac{\gamma \lambda E}{\rho C_p D}. \quad (7)$$

216 G_c was calculated as a daily average conductance using mean daytime T and D, and E
217 summed over 24 hr but divided by daylight hours (Phillips and Oren, 1998; Kumagai et
218 al., 2008). Sap-flux sensors observe water movement through the trunk during nighttime,
219 which may represent recharge of water into upper sections of the tree trunk and branches
220 or transpiration during nighttime. Dividing E by daylight hours assumes that sap flux
221 observed during nighttime represents recharge of water. Recent studies (Dawson et al.,

2007; Fisher et al., 2007; Oishi et al., 2008) have reported that transpiration during nighttime accounts for a considerable portion of daily transpiration. However, transpiration during nighttime would be very low in Japan possibly because of low D during nighttime, as shown by measurements of transpiration using the leaf-chamber method (Kosugi et al., 1995, 1997; Tanaka et al., 2002). The "daytime" here was assumed as the period between 6 a.m. and 6 p.m. throughout the year for simplicity, i.e., the daylight hours were assumed as 12. These assumptions were also made in previous studies (Kumagai et al., 2008; Komatsu et al., 2012). We confirmed that these assumptions did not alter our conclusions. D for the period between 6 a.m. and 6 p.m. differed from D for the period between sunrise and sunset by no more than 8% for our sites. Our preliminary analysis revealed that G_c calculated using D for the period between 6 a.m. and 6 p.m. could differ from those calculated using D for the period between sunset and sunrise by no more than 10%, which was not large enough to alter our conclusions.

We determined G_{cref}, β, and δ for the sites where E data only during the growing season were available. Here, $h(T)$ was assumed to be 1.00 because of relatively high T. We determined G_{cref}, β, δ, ε, and ζ for the sites where year-round E data were available. Note that analysis for the XT site did not follow this policy, as detailed later.

The parameters were determined in a manner similar to that employed by Komatsu et al. (2012, 2013). We first excluded data recorded on rainy days and days with D lower than 0.2 kPa. Data for sap flux (and therefore E and G_c) could suffer from

242 measurement errors on rainy days (Kumagai et al., 2008; Komatsu et al., 2012). G_c could
243 be highly affected by measurement errors in D when D is very low (Ewers and Oren,
244 2000; Komatsu et al., 2007b). We then examined the relationship between D and G_c using
245 data recorded on days with high R (>400 W m^{-2}) and T (>15 °C). We determined G_{cref}
246 and β by regressing the relationship emloying the least-squares method. After
247 determining G_{cref} and β, we examined the relationship between R and observed G_c divided
248 by G_{cref} $f(D)$ using data recorded on days with high T (>15 °C) to determine δ. Here, we
249 confirmed that the relationship between soil water content and observed G_c divided by
250 G_{cref} $f(D)g(R)$ was generally unclear for sites where data for soil water content were
251 available. We finally examined the relationship between T and observed G_c divided by
252 G_{cref} $f(D)g(R)$ to determine ε and ζ. Here, we also confirmed that the relationship between
253 T and observed G_c divided by G_{cref} $f(D)g(R)$ was generally unclear for the sites where E
254 data only during the growing season were available.

255 We applied a different method to the determination of parameters for XT. XT
256 was located in a mountainous region under a humid subtropical climate. If we had applied
257 the same method as that applied to other sites, we would have only limited data with
258 which to examine the relationship between D and G_c because of a large number of rainy
259 days and days with low R. The method applied to XT was as follows. We first excluded
260 data recorded on days with daily rainfall more than 5.0 mm and days with D lower than
261 0.2 kPa. We then examined the relationship between D and G_c using data recorded on

days with R no less than 300 W m^{-2}. We determined G_{cref} and β by regressing the relationship employing the least-squares method. Here, we confirmed that there was no systematic difference in G_c between days without rain and days with rain no more than 5.0 mm. After determining G_{cref} and β, we examined the relationship between R and observed G_c divided by G_{cref} $f(D)$ to determine δ. In the above analysis, we did not exclude data using a criterion about T, because the range of T was narrow for XT and a large portion of the data satisfied T being no less than 15 °C. We did not determine the parameters in $h(T)$, because we did not find a clear relationship between T and observed G_c divided by G_{cref} $f(D)g(R)$ for XT.

4.2. Assessing the importance of parameters

We hypothesized that considering the variation in G_{cref} among the sites would be important but considering variations in β, δ, ε, and ζ among the sites would not be in reproducing E for the 14 sites (detailed in the theory). To verify this hypothesis, we calculated E for days with no rain and T no less than 15 °C (corresponding to a growing season) for the sites using three different parameterizations: (P1G) the mean values of G_{cref}, β, and δ among the sites, (P2G) G_{cref} determined for each site and the mean values of β and δ among the sites, and (P3G) G_{cref}, β, and δ determined for each site. To evaluate the reproducibility of E by P1G, P2G, and P3G, we examined the relationships of the mean E for the days calculated using P1G, P2G, and P3G respectively with the mean

observed E. If the difference in reproducibility between P1G and P2G was found to be important, considering the variation in G_{cref} among the sites would be important in calculating the mean E for a growing season. If the difference in reproducibility between P2G and P3G was found to be unimportant, considering variations in β and δ would not be important.

Similarly, we calculated E for days with no rain for sites having data recorded in winter as well as those recorded in a growing season using three different parameterizations: (P1W) the mean values of G_{cref}, β, δ, ε, and ζ among the sites, (P2W) G_{cref} determined for each site and the mean values of β, δ, ε, and ζ among the sites, and (P3W) G_{cref}, β, δ, ε, and ζ determined for each site. To evaluate the reproducibility of E by P1W, P2W, and P3W, we examined the relationships of the mean E for the days calculated using P1W, P2W, and P3W respectively with the mean observed E. If the difference in reproducibility between P1W and P2W was found to be important, considering the variation in G_{cref} would be important in calculating the mean E for a period including a growing season and winter. If the difference in reproducibility between P2W and P3W was found to be unimportant, considering variations in β, δ, ε, and ζ among the sites would not be important.

When evaluating the model reproducibility, we primarily focused on the mean E on a longer time scale, because our model was intended to be used to improve our understanding of the forest water balance on a long time scale (see Section 1). For

assessing the importance of the difference in reproducibility between different parameterizations, we did not examine whether there was a statistically significant difference between errors in *E* estimates using different parameterizations. What we need to know is not whether there is a statistical difference, but whether the magnitude of the difference is important in a practical context (Bakan, 1966; Thompson, 1996, 1998; Nuzzo, 2014). We thus examined whether errors in estimates of the mean *E* made using the G_c model were less than potential errors in observed *E*. Kumagai et al. (2007) and Kume et al. (2010) examined uncertainty in *E* estimates made using the sap-flux method for Japanese cedar and cypress plantations. Sampling data for sap flux on a sensor scale repeatedly using the Monte-Carlo technique, Kumagai et al. (2007) and Kume et al. (2010) revealed that the standard variation of *E* estimates was generally 10% or more of the mean *E*. When considering that 95% of data theoretically fall in the range of two standard deviations above and below the mean, potential errors in observed *E* would be less than 20% of the value in most cases. If errors in *E* estimates made using different parameterizations were more than 20% of observed *E*, we would regard the difference in reproducibility as important.

In addition, we examined whether errors in estimates of the mean *E* made using the G_c model were less than those in interception evaporation estimates made using the model developed by Komatsu et al. (2007a) or its revised form developed by Komatsu et al. (submitted), because our G_c model was intended to be used with the interception

evaporation model to assess the water balance for Japanese cedar and cypress plantations (Komatsu et al., submitted). The typical errors in interception evaporation estimates for the period with T no less than 15 °C and for a year would be 0.22 and 0.20 mm day^{-1}, respectively (Appendix A).

4.3. Relating important parameters with species and structures

We examined the relationship between A and G_{cref} to model G_{cref} using A. After confirming correlation between the two variables, we regressed the relationship to obtain a linear equation relating G_{cref} with A. The intercept of the equation was assumed to be zero. The slope of the equation was determined employing the least-squares method. To examine the stability of the correlation and the slope, we calculated 95% confidence intervals of these variables employing the bootstrapping method (Efron, 1979; Diaconis and Efron, 1983). These intervals were “bias-corrected, accelerated” percentile intervals calculated in the manner described by Efron (1987) and Fox (2008).

As data for A are not usually available for most Japanese cedar and cypress plantations, we tried to relate A with the mean diameter at breast height (d_m) and stem density (N) data in the following way. Tsuruta et al. (2011) summarized data for the sapwood area at a tree scale (a) for 81 cedar trees from six sites and 109 cypress trees from nine sites and examined the relationships between diameter at breast height (d) and a for these species. They did not find clear differences in the relationship among sites.

They regressed the data to develop general equations for the relationships: $a = a_{ref} \cdot d^k$, where a and d were respectively in units of cm^2 and cm and a_{ref} and k were parameters. a_{ref} was 1.40 and 1.96 cm^2 for cedar and cypress, respectively. k was 1.55 and 1.42 for cedar and cypress, respectively. Approximating this equation by the tangential line at d being equal to d_m, A was expressed as

$$A = N \cdot a_{\mathrm{ref}} \cdot d_m^{\,k}. \quad (8)$$

To examine the validity of this method of estimating A from N and d_m, we investigated the relationship between A estimated employing this method and observed A. For this validation, we used A data for YB, YA, IS, KL, KU, KS, XT, and IH, and another cypress site of Sun et al. (2014). Data for the other six sites (i.e., IK, IR, OL, OU, SK, and HW) were not used, because a data for the sites were used by Tsuruta et al. (2011) to develop the relationship between d and a.

5. Results

5.1. Determination of parameters

Figure 1 shows the relationships between D and G_c, between R and G_c divided by $G_{cref}\, f(D)$, and between T and G_c divided by $G_{cref}\, f(D)\, g(R)$. Here, we show data only for OL as an example. Regressing these relationships and relationships for the other sites, parameters for the sites were determined as listed in Table 2. The maximum G_{cref} (9.77 mm s^{-1} for IK) among the sites was more than five times the minimum G_{cref} (1.76 mm s^{-}

362 ^{1} for IH). We observed variations in $f(D)$, $g(R)$, and $h(T)$ among sites (Figure 2).

363

364 5.2. Assessing the importance of parameters

365 Figure 3 shows the relationships of the mean E for days with no rain and T no
366 less than 15 °C calculated using P1G, P2G, and P3G with observed E. E calculated using
367 the model was not strongly correlated (r = 0.454) with observed E for P1G, but was
368 strongly correlated (r = 0.993 and 0.997, respectively) and fell along the 1:1 line for P2G
369 and P3G. Errors for P1G were often greater than potential errors in observed E and
370 interception evaporation estimates, but errors for P2G and P3G were not. Figure 4 shows
371 the relationships of mean E for days with no rain calculated using P1W, P2W, and P3W
372 with observed E for sites having data recorded in winter as well as those recorded in a
373 growing season. E calculated using the model was not strongly correlated (r = 0.597) with
374 observed E for P1W, but was strongly correlated (r = 0.999 and >0.999, respectively) and
375 fell along the 1:1 line for P2W and P3W. Errors for P1W were often greater than potential
376 errors in observed E and interception evaporation estimates, but errors for P2W and P3W
377 were not. These results suggest that considering the variation in G_{cref} among the sites was
378 important for reproducing the mean E on a long time scale, but considering variations in
379 β, δ, ε, and ζ was not.

380 Besides the mean E on a long time scale, we also examined model reproducibility
381 of seasonal and day-to-day variations in E using data on a daily time scale for sites where

382 year-round data were available. Figure 5 shows time series of E calculated using P1W,
383 P2W, and P3W and observed E. Here, we show data only for OU as an example. The
384 slope of the regression line for the relationship between calculated and observed E often
385 fell outside the range between 0.8 and 1.2 for P1W, where the range corresponded to the
386 uncertainty in observed E. However, the slope always fell in the range for P2W and P3W
387 (Table 3). The determination coefficients for P1W and P2W were often lower than that
388 for P3W. However, the difference was relatively small. These results suggest that
389 considering the variation in G_{cref} among the sites was important for reproducing seasonal
390 and day-to-day variations in E, but considering variations in β, δ, ε, and ζ was not.
391
392 5.3. Relating important parameters with species and structures
393 G_{cref} tended to increase with A (Figure 6). The correlation coefficient (r) was
394 0.698 and the 95% confidence interval was (0.446, 0.951), when pooling data for cedar
395 and cypress. The correlation between A and G_{cref} was stronger than that between L and
396 G_{cref} (r = 0.479). The regression line was determined as $G_{cref} = 0.157\,A$, where A and G_{cref}
397 were in units of $m^2\ ha^{-1}$ and $m\ s^{-1}$, respectively. The 95% confidence interval of the slope
398 was (0.127, 0.195). Data for both cedar and cypress were located along the regression
399 line, suggesting no clear difference in G_{cref} for a given A between cedar and cypress. Thus,
400 the regression equation could be used to predict G_{cref} from A for both cedar and cypress
401 plantations and then to predict E. Figure 7 shows the normal probability plot (Fujii, 2005;

Peck and Devore, 2005) for differences between G_{cref} estimated using the regression equation and observed G_{cref}, where the normal score in the y-axis indicates the difference divided by the standard deviation of the difference for the 14 sites. Data for all sites except SK and IK were approximated by a line, indicating that most of these data followed a normal distribution. However, data for SK and IK were located far from the line, suggesting that observed G_{cref} for these sites was higher than expected from the regression equation and a normal distribution of the differences between estimated and observed G_{cref}.

Figure 8 compares A estimated from N and d_m and observed A. Data were generally located around the 1:1 line. The mean relative error (i.e., the ratio of the difference between estimated and observed A to observed A) was 26%. The magnitude of this error is discussed in Section 6.3.

6. Discussion

6.1. Roles of $f(D)$, $g(R)$, and $h(T)$

Our model succeeded in reproducing E observed for the 14 sites, suggesting validity of our hypothesis. Our model includes three functions, i.e., $f(D)$, $g(R)$, and $h(T)$. These functions influence on calculated E differently. Omitting $f(D)$ from Eq. (2) (i.e., assuming $f(D)$ being 1.0) causes overestimation of E during May–August (Figure 9a), resulting in a relatively low determination coefficient (R^2 = 0.740) for the relationship

between calculated and observed E. This suggests that considering reduction in G_c with increasing D is important in reproducing E when D is high.

Omitting $g(R)$ causes overestimation of E during October–January when R is relatively low. Omitting $h(T)$ causes overestimation of E during January–February when T is relatively low. However, the determination coefficients for these cases (R^2 = 0.792 and 0.798, respectively) are higher than that for the case of omitting $f(D)$. This suggests that effects of omitting $g(R)$ and $h(T)$ on reproducing E on a daily time scale are less important than that of omitting $f(D)$.

6.2. Variability in G_{cref}

G_{cref} values for SK and IK were higher than expected from the regression equation (Figure 7). There are technical factors that potentially affect variations in G_{cref} among sites. An insufficient number of sensors for sap flux measurements could result in large errors in E estimates. Shinohara et al. (2013a) compared errors in E estimates introduced by ignoring tree-to-tree variations, radial variations, and circumference variations in sap flux for a Japanese cedar plantation. They concluded that tree-to-tree variations in sap flux are the primary factor of errors in E estimates. Previous studies (Kumagai et al., 2005, 2007; Kume et al., 2010; Shinohara et al., 2013b) reported that errors in E estimates for Japanese cedar and cypress were serious when the number of trees in which sensors were installed was low, especially when there were less than

approximately 10. Note that this threshold number would be species specific, because different threshold numbers were reported for other species (Oren et al., 1998; Mackay et al., 2010). There were approximately 10 in which sensors were installed at each site (10 for SK and 9 for IK). Furthermore, *E* for IK estimated from sap flux data derived for nine trees differed less than 5% from that estimated from sap flux data derived for all 18 trees according to intensive measurements performed during May 16–18 and June 1–4, 2010 for the site. Thus, the numbers of sensors at these sites are not likely a main factor explaining the higher G_{cref}.

The use of the simplified Penman–Monteith equation could also be a factor causing higher G_{cref}. Aerodynamic conductance, which is assumed as infinite in the simplified Penman–Monteith equation, generally ranges between 70 and 400 mm s^{-1} for coniferous forests including Japanese cedar and cypress plantations (Stewart and Thom, 1973; Yamanoi and Ohtani, 1992; Loustau et al., 1996; Tanaka et al., 1996). When assuming aerodynamic conductance as 70 mm s^{-1} and calculating G_{cref} using the original Penman–Monteith equation (see the methods used by Komatsu et al., 2012), G_{cref} values for SK and IK are determined as 3.53 and 6.22 mm s^{-1}, respectively. These G_{cref} data are located close to the regression line in Figure 6, implying that the use of the simplified Penman–Monteith equation might be a potential factor explaining the higher G_{cref} for the sites. Unfortunately, there have been no data for aerodynamic conductance observed at these sites. However, data for wind speed for IK are available. The relationship between

462 D and G_c differed only slightly according to wind speed, suggesting that low aerodynamic
463 conductance would not be the primary factor causing low G_{cref} for IK. Data for wind speed
464 for SK were unavailable.

465 Besides the factors discussed above, age might be another possible factor
466 explaining high G_{cref} for SK, which is younger than the other sites (Table 1). There have
467 been several studies reporting or suggesting changes in sap flux on a stand scale with age
468 for mono-specific forests (Tsuruta et al., 2008; Forrester et al. 2010). We do not have data
469 for other sites of similar age to SK. We thus recommend examining G_{cref} for young
470 Japanese cedar and cypress plantations.

471

472 6.3. Errors in A estimates

473 We observed a clear correlation between estimated and observed A (Figure 8).
474 However, the error in A estimates was relatively large. The mean relative error in A
475 estimates (26%) was comparable to that in G_{cref} estimates obtained using the regression
476 equation in Figure 5 (24%). Thus, it would be better to use observed A to calculate G_{cref},
477 if observed A is available.

478 The error in A estimates would be primarily caused by errors in a estimates using
479 Tsuruta et al.'s (2011) equation, and only secondarily caused by errors due to tangential
480 approximation of the equation (Eq. (8)). The tangential approximation could cause
481 underestimation of A, because a values calculated using the tangential line are no more

than those calculated using the original equation. In fact, *A* estimated employing the above method did not always underestimate observed *A* (Figure 8).

6.4. Possible applications and implications

Our model would be useful as a research tool for hydrologists. There have been many studies (Dung et al., 2012; Kubota et al., 2013) examining changes in the annual water balance with changing structure of Japanese cedar and cypress plantations due to forest management. There are large variations in the change in the annual water balance among studies. Our model, accompanied with the interception evaporation model developed by Komatsu et al. (2007a), could be used by hydrologists to calculate changes in *E* and interception evaporation for catchments and improve our understanding of underlying processes of the variations. Our model and the interception model are also useful in estimating spatial variations in *E* and interception evaporation on a landscape scale, when these models are used with forest inventory data.

As described above, our model has great potential for application. This is because our model can be used only with the inputs of commonly available data for forest structure (i.e., *N* and d_m) and meteorology (see Appendix B). Our model is specific to Japanese cedar and cypress plantations. However, our model is important in that it demonstrates how to relate *E* with commonly available data. The concept of our model would be useful in developing similar models to estimate *E* for mono-specific forests

comprising other species.

On the other hand, the model needs to be tested further. The sites for cedar and cypress plantations (Table 1) were located mainly in western Japan, where temperature is intermediate or higher in the distribution areas of cedar and cypress (Japan Forestry Agency, 2013). We do not have enough *E* data for cedar and cypress plantations recorded in regions where temperature is lower, except data for IK. The response of G_c to temperature for stands in this region might be different from that observed in this study. We thus recommend testing the applicability of the model using data derived for sites located in this region. Furthermore, it is preferable to test the model applicability using data for sites with various age classes. Ages of the sites (Table 1) ranged between 19 and 99 years, which almost covers the age range for most Japanese cedar and cypress plantations in Japan (Japan Forestry Agency, 2013). However, many of the sites fall in the range of 40–60 years. Thus, applicability of our model has been tested sufficiently for stands within this age class, but has not been fully tested outside the age class. A major portion of Japanese cedar and cypress plantations in Japan falls in this age class, suggesting the practical usefulness of the model. On the other hand, the portion of older stands is expected to increase, because forestry in Japan has stagnated and cedar and cypress plantations have not been actively harvested (Komatsu et al., 2010). Therefore, we recommend testing the applicability of the model to stands outside the age class.

522 Acknowledgements

523 We express our sincere thanks to members of Kyushu University Forest for their
524 dedicated efforts in initiating the sites. We acknowledge Dr. Xinchao Sun (Graduate
525 School of Life and Environmental Sciences, University of Tsukuba, Japan) for providing
526 sapwood-area data for their site. Thanks are also due to two anonymous reviewers for
527 providing critical comments. This research has been supported by a CREST project
528 (Development of Innovative Technologies for Increasing Watershed Runoff and
529 Improving River Environment by the Management Practice of Devastated Forest
530 Plantation).

531

532 Appendix. A. Errors in interception evaporation estimates

533 The interception evaporation model developed by Komatsu et al. (2007a) and its
534 revised form developed by Komatsu et al. (submitted) typically have an error of 4% of
535 incident rainfall. The period with T no less than 15 °C is typically April–October in
536 regions where Japanese cedar and cypress are distributed and incident rainfall during the
537 period is typically 1200 mm (National Astronomical Observatory, 2013). Annual rainfall
538 in the regions is typically 1800 mm. Thus, the typical error in interception evaporation
539 estimates for the period with T no less than 15 °C would be 48 mm, which was equivalent
540 to 0.22 mm day^{-1}. The typical error for a year would be 72 mm, which was equivalent to
541 0.20 mm day^{-1}.

542

543 Appendix. B. Methods of preparing meteorological inputs

544 The model developed in this study requires daytime (6 a.m.–6 p.m.) mean solar
545 radiation (R), temperature (T), and vapor pressure deficit (D) as meteorological inputs. R
546 data are not always available throughout Japan (Shinohara et al., 2007). It is often the
547 case that only daily maximum (T_x) and minimum temperatures (T_n) are available for
548 historical data (The University of Tokyo Forests, 2014).

549 The former problem can be solved by substituting R for the target area by data
550 for solar radiation recorded at a meteorological observatory in surrounding areas. Data
551 for daily solar radiation are recorded at main meteorological observatories in Japan (Japan
552 Meteorological Agency, 2014). R in units of W m^{-2} can be approximated by daily solar
553 radiation in units of MJ m^{-2} day^{-1} multiplied by an index of 23.1, which converts the units.
554 E during January 1–December 31, 2008 calculated using the model with the input of R,
555 T, and D observed at OL is 234 mm. Here, G_{cref} is assumed to be 0.00322 m s^{-1} on the
556 basis of observed A and the relationship between A and G_{cref} (Figure 6). E values during
557 the same period calculated with the input of solar radiation observed at meteorological
558 observatories at Fukuoka, Saga, Oita, and Hiroshima are 238, 234, 237, and 240 mm,
559 respectively. These meteorological observatories are located 15, 50, 110, 200 km from
560 OL, respectively. All these values approximate the value calculated using R for OL.
561 Qualitatively, the same results are available for other sites. Thus, accurate estimates of R

562 are not important for estimating E using the model. This is attributed to E being
563 insensitive to R when R is high (Figure 2b) and E on days with high R accounting for a
564 relatively large portion of annual E.

565 The latter problem (i.e., only T_x and T_n are available) can be solved making the
566 following assumptions. First, the diurnal trend in temperature is approximated using a
567 sine function minimized at 6 a.m. and maximized at 2 p.m. A simliar approximation has
568 been commonly used to produce hourly temperature data from T_x and T_n (Campbell and
569 Norman, 1998). Under this assumption, T (i.e., temperature during 6 a.m.–6 p.m.) is
570 analytically written as $T = (T_x + T_n)/2 + (T_x - T_n)/(3\pi)$. Second, vapor pressure deficit at
571 6 a.m. is zero and daytime vapor pressure deficit is caused by a temperature rise during
572 the day. Note that the assumption of vapor pressure deficit being zero in the morning is
573 generally valid except in arid and semi-arid regions (Running et al., 1987; Kimball et al.,
574 1994). D (i.e., the mean vapor pressure deficit during 6 a.m.–6 p.m.) is thus approximated
575 by $D = e_s(T) - e_s(T_n)$, where e_s is the saturation vapor pressure. E during January 1–
576 December 31, 2008 calculated using the model with the input of R, T, and D observed at
577 OL is 234 mm. E during the same period calculated with the input of R, T_x and T_n observed
578 at OL is 225 mm, which approximates E calculated with the input of T and D.
579 Qualitatively, the same results are available for other sites.

References

Adams, K.N., Fowler, A.M., 2006. Improving empirical relationships for predicting the effect of vegetation change on annual water yield. J. Hydrol. 321, 90–115.

Addington, R.N., Mitchell, R.J., Oren, R., Donovan, L.A., 2004. Stomatal sensitivity to vapor pressure deficit and its relationship to hydraulic conductance in *Pinus palustris*. Tree Physiol. 24, 561–569.

Bakan, D., 1966. The test of significance in psychological research. Psychol. Bull. 66, 423–437.

Baldocchi, D., Meyers, T.P., 1998. On using eco-physiological, micrometeorological and biogeochemical theory to evaluate carbon dioxide, water vapor and trace gas fluxes over vegetation: a perspective. Agric. For. Meteorol. 90, 1–25.

Bosch, J.M., Hewlett, J.D., 1982. A review of catchment experiments to determine the effect of vegetation changes on water yield and evapotranspiration. J. Hydrol. 55, 3–23.

Bréda, N.J.J., 2003. Ground-based measurements of leaf area index: a review of methods, instruments and current controversies. J. Exp. Bot. 54, 2403–2417.

Brown, A., Zhang, L., McMahon, T.A., Western, A.W., Vertessy, R.A., 2005. A review of paired catchment studies for determining changes in water yield resulting from alterations in vegetation. J. Hydrol. 310, 28–61.

Campbell, G.S., Norman, J.M., 1998. An Introduction to Environmental Biophysics.

600 Springer-Verlag, New York.

601 Cienciala, E., Eckersten, H., Lindroth, A., Hallgren, J., 1994a. Simulated and measured
602 water uptake by *Picea abies* under non-limiting soil water conditions. Agric. For.
603 Meteorol. 71, 147–164.

604 Cienciala, E., Lindroth, A., Cermak, J., Hallgren, J., Kucera, J., 1994b. The effects of
605 water availability on transpiration, water potential and growth of *Picea abies* during a
606 growing season. J. Hydrol. 155, 57–71.

607 Cornish, P.M., Vertessy, R.A., 2001. Forest age-induced changes in evapotranspiration
608 and water yield in a eucalypt forest. J. Hydrol. 242, 43–63.

609 Dawson, T.E., Burgess, S.S.O., Tu, K.P., Oliveira, R.S., Santiago, L.S., Fisher, J.B.,
610 Simonin, K.A., Ambrose, A.R., 2007. Nighttime transpiration in woody plants from
611 contrasting ecosystems Tree Physiol. 27, 561–575.

612 Diadonis, P., Efron, B., 1983. Computer-intensive methods in statistics. Sci. Am. 248,
613 116–131.

614 Domec, J.C., Ogée, J., Noormets, A., Jouangy, J., Gavazzi, M., Treasure, E., Sun, G.,
615 McNulty, S.G., King, J.S., 2012. Interactive effects of nocturnal transpiration and
616 climate change on the root hydraulic redistribution and carbon and water budgets of
617 southern United States pine plantations. Tree Physiol. 32, 707–723.

618 Dung, B.X., Gomi, T., Miyata, S., Sidle, R.C., Kosugi, K., Onda, Y., 2012. Runoff
619 responses to forest thinning at plot and catchment scales in a headwater catchment

draining Japanese cypress forest. J. Hydrol. 444–445, 51–62.

Efron, B., 1979. Bootstrap methods: another look at the Jacknife. Ann. Stat. 7, 1–26.

Efron, B., 1987. Better bootstrap confidence intervals. J. Amer. Statis. Assoc. 82, 171–185.

Ewers, B.E., Oren, R., 2000. Analyses of assumptions and errors in the calculation of stomatal conductance from sap flux measurements. Tree Physiol. 20, 579–589.

Ewers, B.E., Mackay, D.S., Tang, J., Bolstad, P.V., Samanta, S., 2008. Intercomparison of sugar maple (*Acer saccharum* Marsh.) stand transpiration responses to environmental conditions from the Western Great Lakes Region of the United States. Agric. For. Meteorol. 148, 231–246.

Ewers, B.E., Bond-Lamberty, B., Machay, D.S., 2011. Consequences of stand age and species' functional trait changes on ecosystem water use of forests, in Meinzer, F.C., Lachenbruch, B., Dawson, T.E. (Eds.), Size- and Age-Related Changes in Tree Structure and Function. Springer, Dordrecht, pp. 481–505.

Fisher, J.B., Baldocchi, D.D., Misson, L., Dawson, T.E., Goldstein, A.H., 2007. What the towers don't see at night: nocturnal sap flow in trees and shrubs at two AmeriFlux sites in California. Tree Physiol. 27, 597–610.

Forrester, D.I., Collopy, J.J., Morris, J.M., 2010. Transpiration along an age series of *Eucalyptus globulus* plantations in southeastern Australia. Forest Ecol. Manage. 259, 1754–1760.

640 Fox, J., 2008. Applied Regression Analysis and Generalized Linear Models. Sage
641 Publications, Thousand Oaks, Carfornia.
642 Franzer, G.W., Ganha, C.D., Lerzman, K.P., 1999. Gap Light Analyzer (GLA) Version
643 2.0: Image software to Extract Canopy Structure and Gap Light Transmission Indices
644 from True-colour Fisheye Photographs. Simon Franser University, British Columbia,
645 and the Institute of Ecosystem Studies, Millbrook, NewYork, pp. 1–36.
646 Fujii, H., 2005. Practical Methods of Data Analysis for Engineers. Tokyo-Kagaku-Dojin,
647 Tokyo.
648 Granier, A., 1987. Evaluation of transpiration in a Douglas-fir stand by means of sap flow
649 measurements. Tree Physiol. 3, 309–320.
650 Granier, A., Bréda, N., 1996. Modelling canopy conductance and stand transpiration of
651 an oak forest from sap flow measurements. Ann. Sci. For. 53, 537–546.
652 Granier, A., Loustau, D., Bréda, N., 2000a. A generic model of forest canopy conductance
653 dependent on climate, soil water availability and leaf area index. Ann. For. Sci. 57,
654 755–765.
655 Granier, A., Biron, P., Lemoine, D., 2000b. Water balance, transpiration and canopy
656 conductance in two beech stands. Agric. For. Meteorol. 100, 291–308.
657 Hasegawa, K., Omi, H., Hiruma, Y., Kumagai, S., Yamamoto, R., Izumi, T., Matsuyama,
658 H., 2013. Estimation of leaf area index of *Cryptomeria japonica* using various
659 methods : A case study of Aso District, Kumamoto Prefecture. J. Geograph. 122, 875−

891.

Hattori, S., Chikaarashi, H., Takeuchi, N., 1982. Measurement of the rainfall interception and its micrometeorological analysis in a Hinoki stand. Bull. FFPRI 318, 79–102.

Ichihashi, R., Komatsu, H., Kume, T., Onozawa, Y., Shinohara, Y., Tsuruta, K., Otsuki, K., Stand-scale transpiration of two Moso bamboo stands with different culm densities. Ecohydrol. In press.

Japan Forestry Agency, 2013. White Paper for Forest and Forestry. Japan Forestry Agency, Tokyo. (Available at: http://www.rinya.maff.go.jp/j/kikaku/hakusyo/index.html).

Japan Forestry Agency, 2014. Data for Japanese cedar and cypress plantations. http://www.rinya.maff.go.jp/j/sin_riyou/kafun/data.html.

Japan Meteorological Agency, 2014. Meteorological statistics. http://www.jma.go.jp/jma/menu/report.html.

Jarvis, P.G., 1976. The interpretation of the variations in leaf water potential and stomatal conductance found in canopies in the field. Phil. Trans. R. Soc. Lond. B 273, 593–610.

Jarvis, P.G., McNaughton, K.G., 1986. Stomatal control of transpiration: scaling up from leaf to region. Adv. Ecol. Res. 15, 1–49.

Kimball, J.S., Running, S.W., Nemani, R. 1994. An improved method for estimating surface humidity from daily minimum temperature. Agric. For. Meteorol. 85, 87–98.

Komatsu, H., 2004. A general method of parameterizing the big-leaf model to predict the dry-canopy evaporation rate of individual coniferous forest stands. Hydrol. Process.

18, 3019–3036.

Komatsu, H., Kang, Y., Kume, T., Yoshifuji, N., Hotta, N., 2006. Transpiration from a *Cryptomeria japonica* plantation, part 2: responses of canopy conductance to meteorological factors. Hydrol. Process. 20, 1321–1334.

Komatsu, H., Tanaka, N., Kume, T., 2007a. Do coniferous forests evaporate more water than broad-leaved forests in Japan? J. Hydrol. 336, 361–375.

Komatsu, H., Hotta, N., Kume, T., 2007b. What is the best way to represent surface conductance for a range of vegetated sites? Hydrol. Process. 21, 1142–1147.

Komatsu, H., Katayama, A., Hirose, S., Kume, A., Higashi, N., Ogawa, S., Otsuki, K., 2007c. Reduction in soil water availability and tree transpiration in a forest with pedestrian trampling. Agric. Forest Meteorol. 146, 107–114.

Komatsu, H., Kume, T., Otsuki, K., 2007d. Contemporary role of catchment water balance data for forest evapotranspiration research. J. Jpn. For. Soc. 89, 346–359.

Komatsu, H., Kume, T., Otsuki, K., 2010. Water resource management in Japan—forest management or dam reservoirs? J. Environ. Manage. 91, 814–823.

Komatsu, H., Kume, T., Otsuki, K., 2011. Increasing annual runoff–broadleaf or coniferous forests? Hydrol. Process. 25, 302–318.

Komatsu, H., Onozawa, Y., Kume, T., Tsuruta, K., Shinohara, Y., Otsuki, K., 2012. Canopy conductance for a Moso bamboo (*Phyllostachys pubescens*) forest in western Japan. Agric. For. Meteorol. 156, 111–120.

Komatsu, H., Shinohara, Y., Nogata, M., Tsuruta, K., Otsuki, K., 2013. Changes in canopy transpiration due to thinning of a *Cryptomeria japonica* plantation. Hydrol. Res. Lett. 7, 60–65.

Komatsu, H., Shinohara, Y., Otsuki, K., Models to predict changes in annual runoff with thinning and clearcutting of Japanese cedar and cypress plantations in Japan. Submitted to Hydrol. Process.

Kosugi, Y., Kobashi, S., Shibata, S., 1995. Modeling stomatal conductance on leaves of several temperate evergreen broad-leaved trees. J. Jap. Reveget. Tech. 20, 158–167.

Kosugi, Y., Shibata, S., Matsui, K., Kobashi, S., 1997. Differences between deciduous and evergreen broad-leaved trees in the pattern of seasonal change of leaf-scale photosynthetic net assimilation rate and transpiration rate. J. Jap. Reveget. Tech. 22, 205–215.

Kosugi, Y., Takanashi, S., Tanaka, H., Ohkubo, S., Tani, M., Yano, M., Katayama, T., 2007. Evapotranspiration over a Japanese cypress forest. I. Eddy covariance fluxes and surface conductance characteristics for 3 years. J. Hydrol. 337, 269– 283.

Kubota, T., Tsuboyama, Y., Nobuhiro, T., Sawano, S., 2013. Change of evapotranspiration due to stand thinning in the Hitachi Ohta Experimental Watershed. J. Jpn. For. Soc. 95, 37–41.

Kumagai, T., Aoki, S., Nagasawa, H., Mabuchi, T., Kubota, K., Inoue, S., Utsumi, Y. and Otsuki, K., 2005. Effects of tree-to-tree and radial variations on sap flow estimates of

720 transpiration in Japanese cedar. Agric. For. Meteorol. 135, 110–116.

721 Kumagai, T., Aoki, S., Shimizu, T., Otsuki, K., 2007. Sap flow estimates of stand
722 transpiration at two slope positions in a Japanese cedar forest watershed. Tree Physiol.
723 27, 161–168.

724 Kumagai, T., Tateishi, M., Shimizu, T., Otsuki, K., 2008. Transpiration and canopy
725 conductance at two slope positions in a Japanese cedar forest watershed. Agric. For.
726 Meteorol. 148, 1444–1455.

727 Kumagai, T., Tateishi, M., Miyazawa, Y., Kobayashi, M., Yoshifuji, N., Komatsu, H.,
728 Shimizu, T., 2014. Estimation of annual forest evapotranspiration from a coniferous
729 plantation watershed in Japan (1): Water use components in Japanese cedar stands. J.
730 Hydrol. 508, 66–76.

731 Kume, T., Tsuruta, K., Komatsu, H., Kumagai, T., Higashi, N., Shinohara, Y., Otsuki, K.,
732 2010. Effects of sample size on sap flux-based stand-scale transpiration estimates Tree
733 Physiol. 30, 129–138.

734 Kume, T., Tsuruta, K., Komatsu, H., Shinohara, Y., Katayama, A., Ide, J., Otsuki, K.,
735 Differences in sap flux based stand transpiration between upper and lower slope
736 positions in a Japanese cypress plantation watershed. Submitted to J. Hydrol.

737 Laplace 2013. Study on Transpiration in a Taiwanese Moso Bamboo Forest using Sap
738 Flow Measurement. Master thesis, National Taiwan University.

739 Lohammer, T., Linder, S., Falk, O., 1980. FAST-simulation models of gaseous exchange

740 in Scots. Pine. Ecol. Bull. (Stockholm) 32, 505–523.

741 Loustau, D., Berbigier, P., Roumagnac, P., Arruda-Pacheco, C., David, J.S., Ferreira, M.I.,

742 Pereira, J.S., Tavares, R., 1996. Transpiration of a 64-year-old maritime pine stand in

743 Portugal. 1. Seasonal course of water flux through maritime pine. Oecologia 107, 33–

744 42.

745 Macfarlane, C., Bond, C., White, D.A., Grigg, A.H., Ogdena, G.N., Silberstein, R., 2010.

746 Transpiration and hydraulic traits of old and regrowth eucalypt forest in southwestern

747 Australia. Forest Ecol. Manage. 260, 96–105.

748 Mackay, D.S., Ewers, B.E., Loranty, M.M., Kruger, E.L., 2010. On the representativeness

749 of plot size and location for scaling transpiration from trees to a stand. J. Geophys.

750 Res. 115, G02016.

751 McDowell, N.G., Fisher, R.A., Xu, C., Domec, J.C., Hölttä, T., Mackay, D.S., Sperry, J.S.,

752 Boutz, A., Dickman, L., Gehres, N., Limousin, J.M., Macalady, A., Martínez-Vilata,

753 J., Mencuccini, M., Plaut, J.A., Ogée, J., Pangle, R.E., Rasse, D.P., Ryan, M.G.,

754 Sevanto, S., Waring, R.H., Williams, A.P., Yepez, E.A., Pockman, W.T., 2013.

755 Evaluating theories of drought-induced vegetation mortality using a multimodel–

756 experiment framework. New Phytol. 200, 304–321.

757 McNaughton, K.G., Black, T.A., 1973. A study of evapotranspiration from a Douglas fir

758 forest using the energy balance approach. Water Resour. Res. 9, 1579–1590.

759 National Astronomical Observatory, 2013. Chronological Scientific Tables 2014.

760 Maruzen, Tokyo.

761 Nuzzo, R., 2014. Statistical errors. Nature 506, 150–152.

762 Oishi, A.C., Oren, R., Stoy, P.C., 2008. Estimating components of forest
763 evapotranspiration: A footprint approach for scaling sap flux measurements. Agric.
764 For. Meteorol. 248, 1719–1732.

765 Oren, R., Phillips, N., Katul, G., Ewers, B.E., Pataki, D.E., 1998. Scaling xylem sap flux
766 and soil water balance and calculating variance: a method for partitioning water flux
767 in forests. Ann. Sci. For. 55, 191–216.

768 Oren, R., Sperry, J.S., Katul, G.G., Pataki, D.E., Ewers, B.E., Phillips, N., Schäfer, K.V.R.,
769 1999. Survey and synthesis of intra- and interspecific variation in stomatal sensitivity
770 to vapour pressure deficit. Plant Cell Environ. 22, 1515–1526.

771 Peck, R., Devore, J.L., 2005. Statistics: the Exploration and Analysis of Data, Second
772 Edition. Brooks/Cole, Boston, Massachusetts.

773 Phillips, N., Oren, R., 1998. A comparison of daily representations of canopy conductance
774 based on two conditional time averaging methods and the dependence of daily
775 conductance on environmental factors. Ann. Sci. For. 55, 217–235.

776 Running, S.W., Nemani, R.R. and Hungerford, R.D., 1987. Extrapolation of synoptic
777 meteorological data in mountainous terrain, and its use for simulating forest
778 evapotranspiration. Can. J. For. Res. 17, 472–483.

779 Scott, D.F., Lesch, W., 1997. Streamflow responses to afforestation with *Eucalyptus*

780 *grandis* and *Pinus petula* and to felling in the Mokobulaan experimental catchments,
781 South Africa. J. Hydrol. 199, 360–377.
782 Shinohara, Y., Komatsu, H., Otsuki, K., 2007. A method for estimating global solar
783 radiation from daily maximum and minimum temperatures: Its applicability to Japan.
784 J. Jpn. Soc. Hydrol. Water Resour. 20, 462–469.
785 Shinohara, Y., Tsuruta, K., Ogura, A., Noto, F., Komatsu, H., Otsuki, K., Maruyama, T.,
786 2013a. Azimuthal and radial variations in sap flux density and effects on stand-scale
787 transpiration estimates in a Japanese cedar forest. Tree Physiol. 33, 550–558.
788 Shinohara, Y., Tsuruta, K., Kume, T., Otsuki, K., 2013b. An overview of stand-scale
789 transpiration measurements using the sap flow technique for evaluating the effects of
790 forest management practices. J. Jpn. For. Soc. 95, 321–331.
791 Stewart, J.B., Thom, A.S., 1973. Energy budgets in pine forest. Quart. J. Roy. Met. Soc.
792 99, 154–170.
793 Sun, X., Onda, Y., Kato, H., Otsuki, K., Gomi, T., 2014. Partitioning of the total
794 evapotranspiration in a Japanese cypress plantation during the growing season.
795 Ecohydrol. 7, 1042–1053.
796 Suzuki, M., 1980. Evapotranspiratoin from a small catchment in hilly mountains (I)
797 Seasonal variations in evapotranspiration, rainfall interception and transpiration. J. Jpn.
798 For. Soc. 62, 46–53.
799 Tanaka, K., Tanaka, H., Nakamura, A., Ohte, N., Kobashi, S., 1996. Conductance at a

community level and characteristics of CO_2 exchange in hinoki (*Chamaecyparis obtusa*) stand. J. Jpn. For. Soc. 78, 266–272.

Tanaka, K., Kosugi, Y., Nakamura, A., 2002. Impact of leaf physiological characteristics on seasonal variation in CO_2, latent and sensible heat exchanges over a tree plantation. Agric. For. Meteorol. 114, 103–122.

Tanaka, N., Kuraji, K., Shiraki, K., Suzuki, Y., Suzuki, M., Ohta, T., Suzuki, M., 2005. Throughfall, stemflow and rainfall interception at mature *Cryptomeria japonica* and *Chamaecyparis obtusa* stands in Fukuroyamasawa watershed. Bull. Tokyo Univ. Forest 113, 197–240.

The University of Tokyo Forests, 2014. Meteorological data. http://www.uf.a.u-tokyo.ac.jp/eri/public.html.

Thompson, B., 1996. AERA editorial policies regarding statistical significance testing: three suggested reforms. Educational Res. 25, 26–30.

Thompson, B., 1998. Statistical significance and effect size reporting: Portrait of a possible future. Res. Sch. 5, 33–38.

Tsuruta, K., Kume, T., Komatsu, H., Higashi, N., Kumagai, T., Otsuki, K., 2008. Relationship between tree height and transpiration for individual Japanese Cypress (*Chamaecyparis obtusa*). J. Jpn. Soc. Hydrol. Water Resour. 21, 414–422.

Tsuruta, K., Komatsu, H., Shinohara, Y., Kume, T., Ichihashi, R., Otsuki, K., 2011. Allometric equations between stem diameter and sapwood area of Japanese cedar and

820 Japanese cypress for stand transpiration estimates using sap flow measurement. J. Jpn.
821 Soc. Hydrol. Water Resour. 24, 261–270.
822 Tsuruta, K., Nogata, M., Shinohara, Y., Komatsu, H., Otsuki, K., 2014. The correction
823 coefficient for leaf area index measurement based on the optical method in a Japanese
824 cedar (*Cryptomeria japonica*) forest. Bull. Kyushu Univ. For. Accepted.
825 Tsuruta, K., Komatsu, H., Kume, T., Shinohara, Y., Otsuki, K., Canopy transpiration in
826 two Japanese cypress forests with contrasting structures. Submitted to J. For. Res.
827 Xiang Y, Tateishi M, Saito T, Otsuki K, Kasahara T., Changes in canopy transpiration of
828 Japanese cypress and Japanese cedar plantations due to selective thinning. Submitted
829 to Hydrol. Process.
830 Yamanoi, K., Ohtani, Y., 1992. Eddy correlation measurements of energy budget and
831 characteristics of evapotranspiration above a hinoki stand. J. Jpn. For. Soc. 74, 221–
832 228.
833 Zwieniecki, M.A., Holbrook, N.M., 1998. Diurnal variation in xylem hydraulic
834 conductivity in white ash (*Fraxinus americana* L.), red maple (*Acer rubrum* L.) and
835 red spruce (*Picea rubens* Sarg.). Plant, Cell Environ. 21, 1173–1180.

836 Figure captions

837 Figure 1. Relationships (a) between vapor pressure deficit (D) and canopy conductance
838 (G_c), (b) between solar radiation (R) and G_c divided by G_{cref} $f(D)$, and (c) between
839 temperature (T) and G_c divided by G_{cref} $f(D)g(R)$ for the OL site. Solid lines in Figures 1a,
840 1b, and 1c indicate $f(D)$, $g(R)$, and $h(T)$ for OL, respectively. G_{cref} is the reference value
841 of canopy conductance. $f(D)$, $g(R)$, and $h(T)$ are functions expressing the responses of G_c
842 to D, R, and T.

843

844 Figure 2. Functions expressing the responses of canopy conductance to (a) vapor pressure
845 deficit ($f(D)$), (b) solar radiation ($g(R)$), and (c) temperature ($h(T)$) for each site.

846

847 Figure 3. Relationships of the mean transpiration (E) for days with no rain and
848 temperature being no less than 15 °C (i.e., corresponding to a growing season) calculated
849 using (a) P1G, (b) P2G, and (c) P3G with the mean observed E. Here, P1G, P2G, and
850 P3G respectively use the mean values of G_{cref}, β, and δ among the sites, G_{cref} determined
851 for each site and the mean values of β and δ among the sites, and G_{cref}, β, and δ determined
852 for each site. The solid line indicates the 1:1 relationship. Dotted lines indicate conditions
853 that errors in E estimates equal potential errors in observed E. Error bars indicate standard
854 deviations.

855

856 Figure 4. Relationships of the mean transpiration (E) for days with no rain calculated
857 using (a) P1W, (b) P2W, and (c) P3W with the mean observed E for sites having data
858 recorded in winter as well as those recorded in a growing season. Here, P1W, P2W, and
859 P3W respectively use the mean values of G_{cref}, β, δ, ε, and ζ among the sites, G_{cref}
860 determined for each site and the mean values of β, δ, ε, and ζ among the sites, and G_{cref},
861 β, δ, ε, and ζ determined for each site. The solid line indicates the 1:1 relationship. Dotted
862 lines indicate conditions that errors in E estimates equal potential errors in observed E.
863 Error bars indicate standard deviations.
864
865 Figure 5. Time series of daily transpiration (E) calculated using P1W, P2W, and P3W and
866 observed E for OU. Lines for P2W and P3W overlap each other. E observed on rainy days
867 is not plotted in this figure.
868
869 Figure 6. Relationship between the sapwood area at a stand scale (A) and the reference
870 value of canopy conductance (G_{cref}). The regression line for the relationship between A
871 and G_{cref}, determined using the least-squares method, is written as $y = 0.157\ x$.
872
873 Figure 7. Normal probability plot for the difference between estimated and observed
874 reference values of canopy conductance (G_{cref}). The solid line is the regression line,
875 determined using the least-squares method, for all data except those for SK and IK.

876

877 Figure 8. Comparison between estimated and observed sapwood areas on a stand scale
878 (A). The solid line indicates the 1:1 relationship.

879

880 Figure 9. Time series of daily transpiration (E) calculated using P2W by omitting
881 functions expressing the responses of G_c to (a) vapor pressure deficit ($f(D)$), (b) solar
882 radiation ($g(R)$), and (c) temperature ($h(T)$).

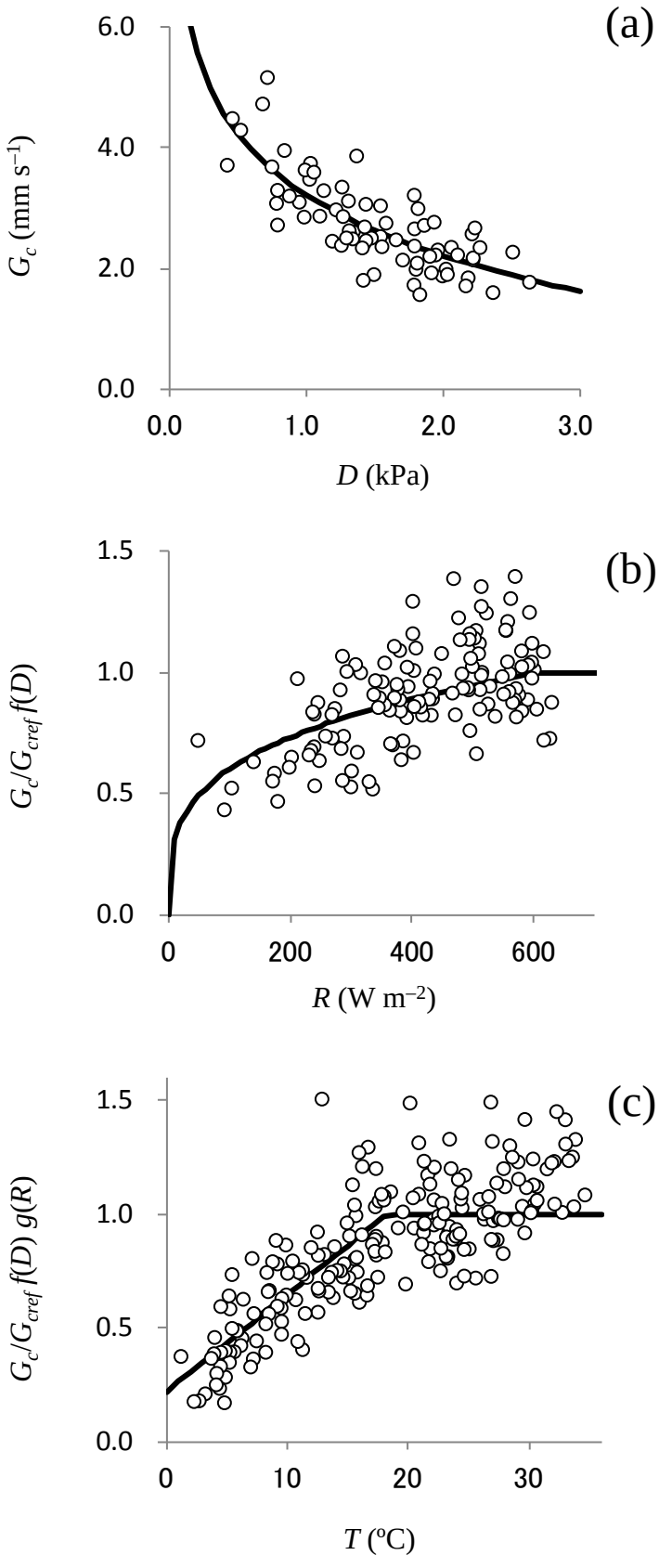

Figure 1

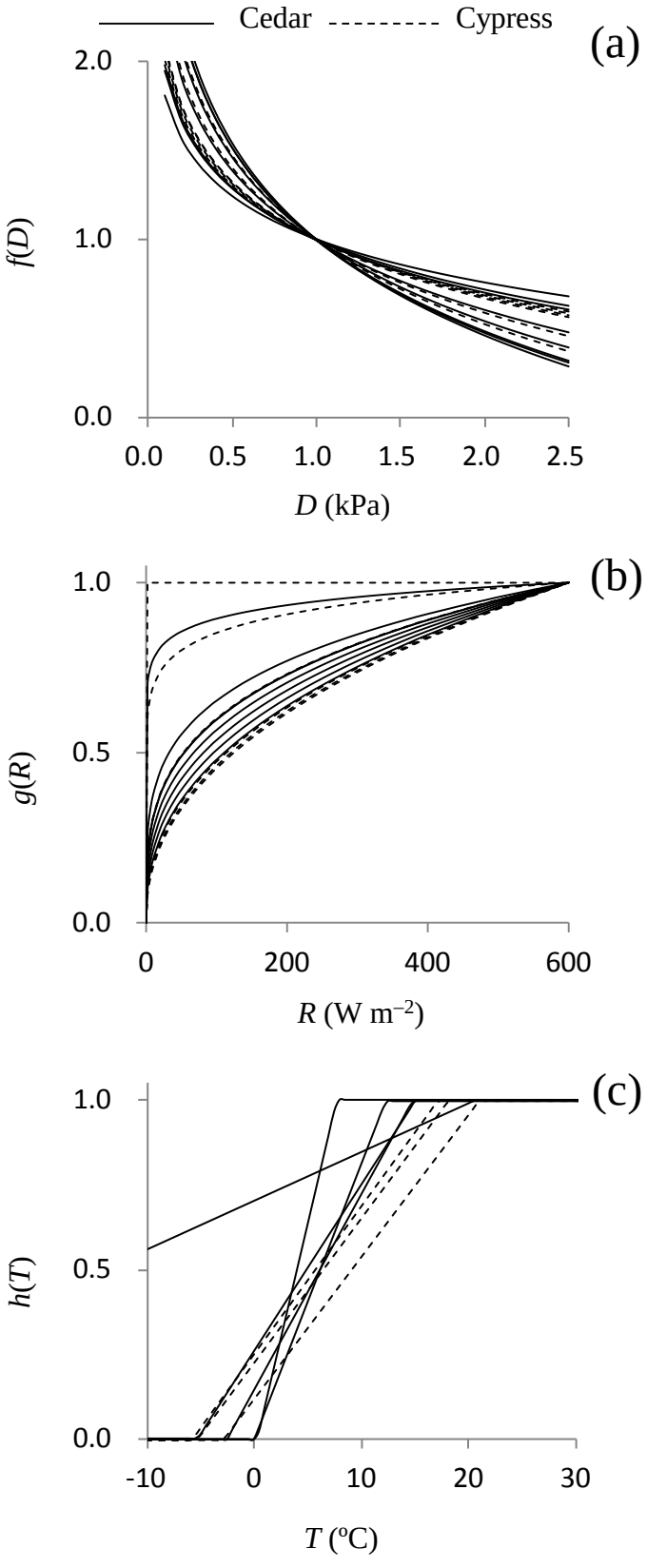

Figure 2

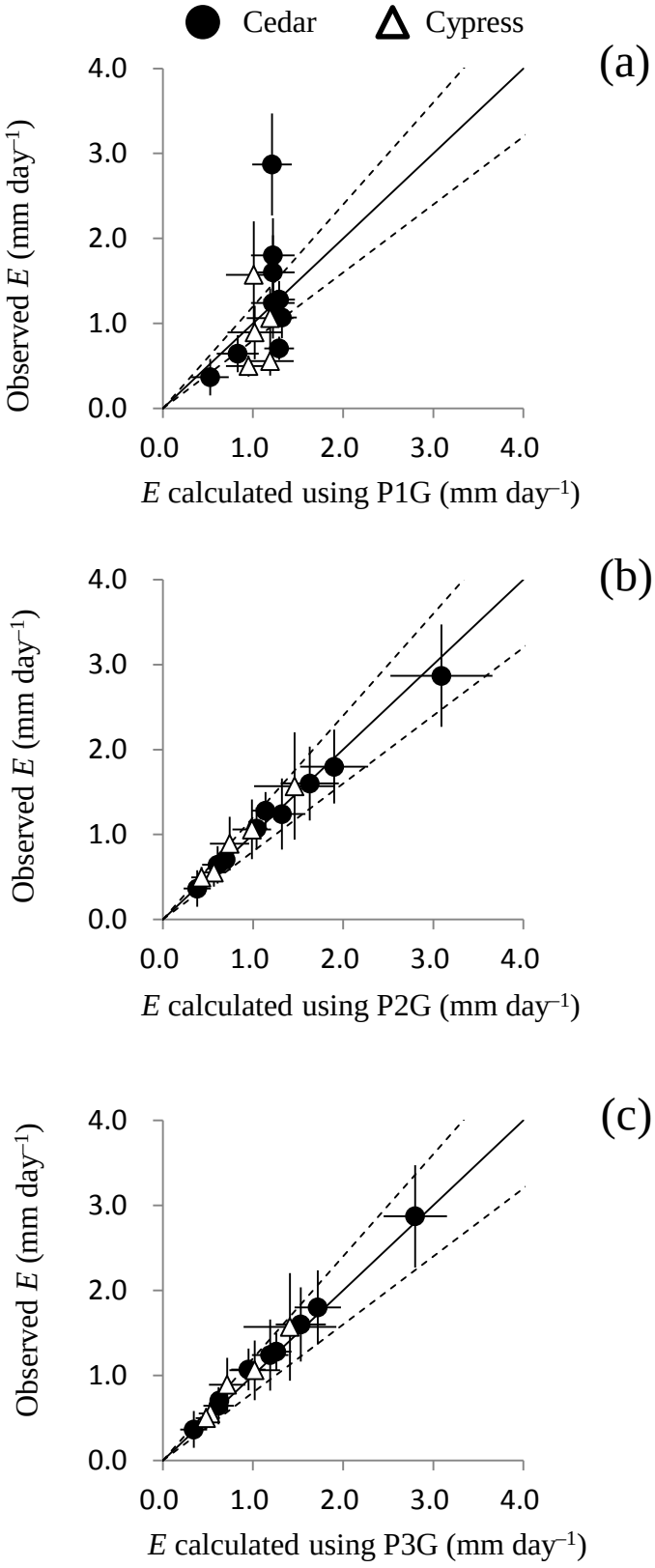

Figure 3

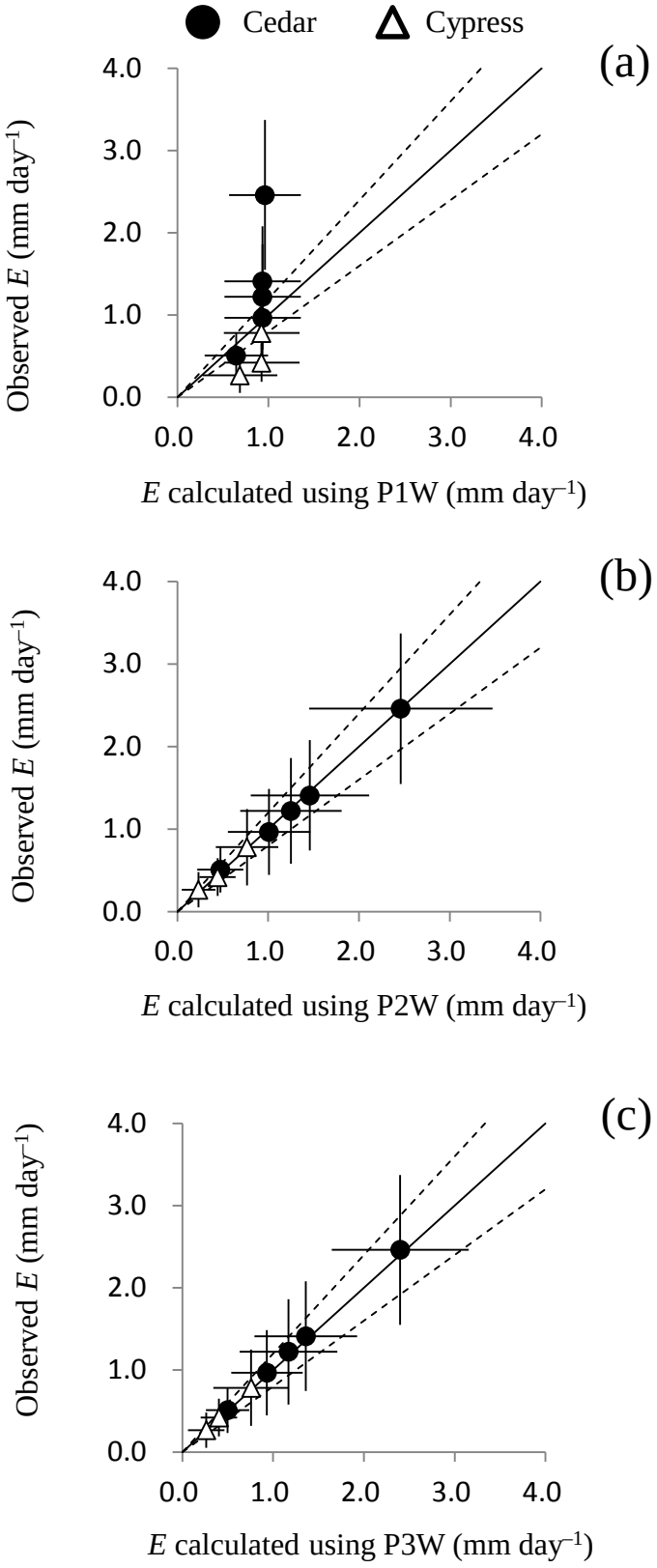

Figure 4

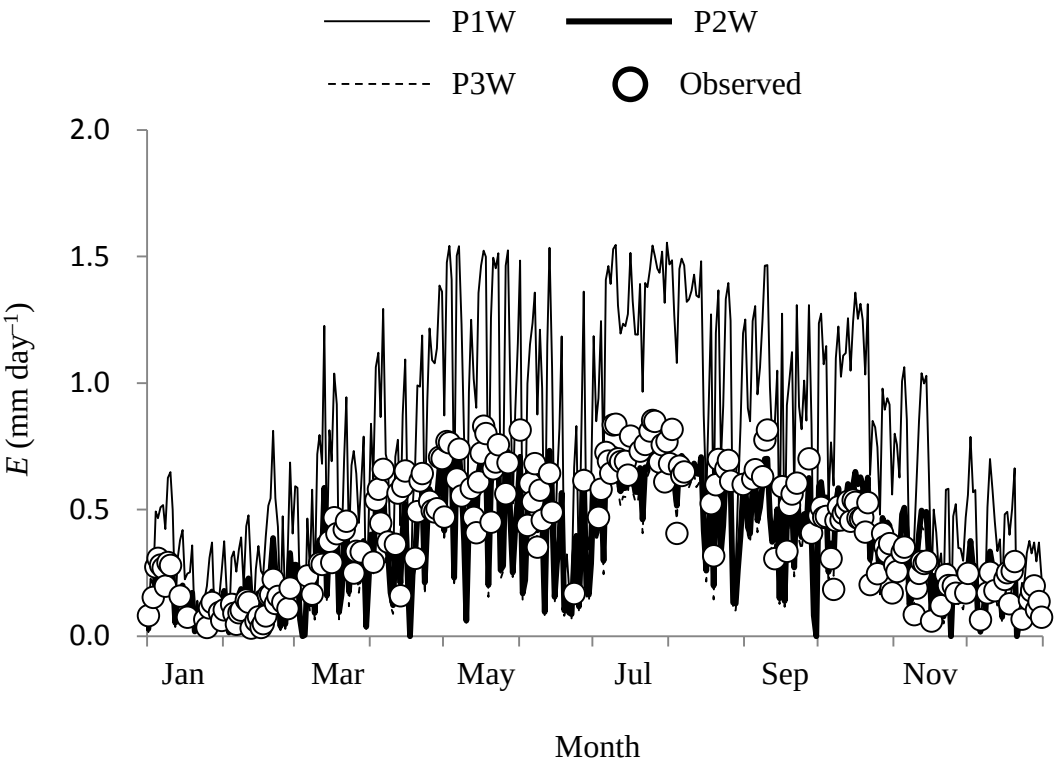

Figure 5

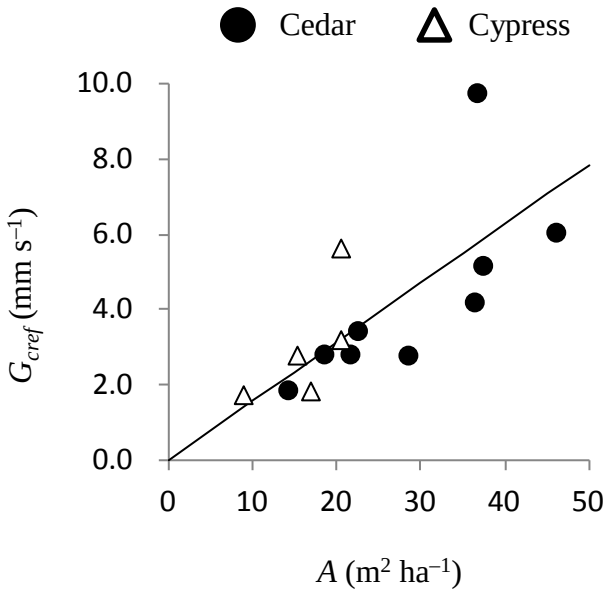

Figure 6

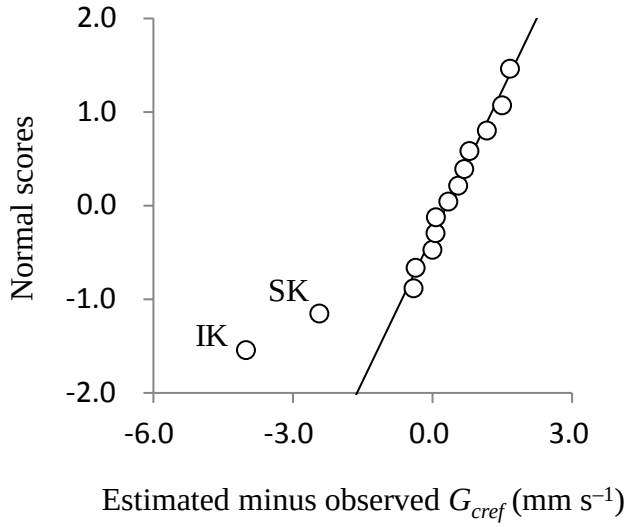

Figure 7

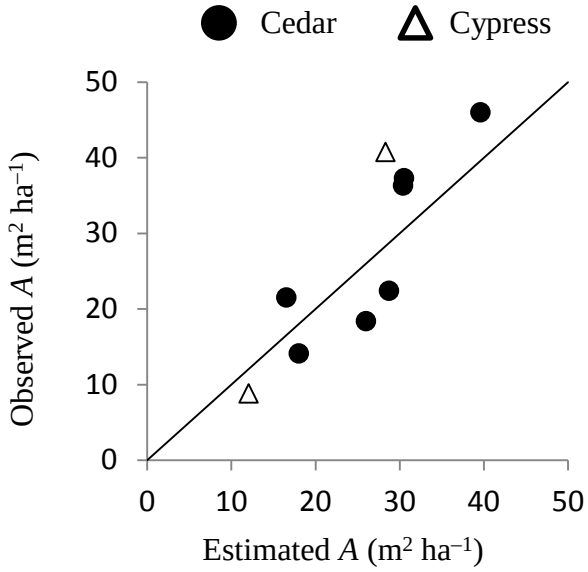

Figure 8

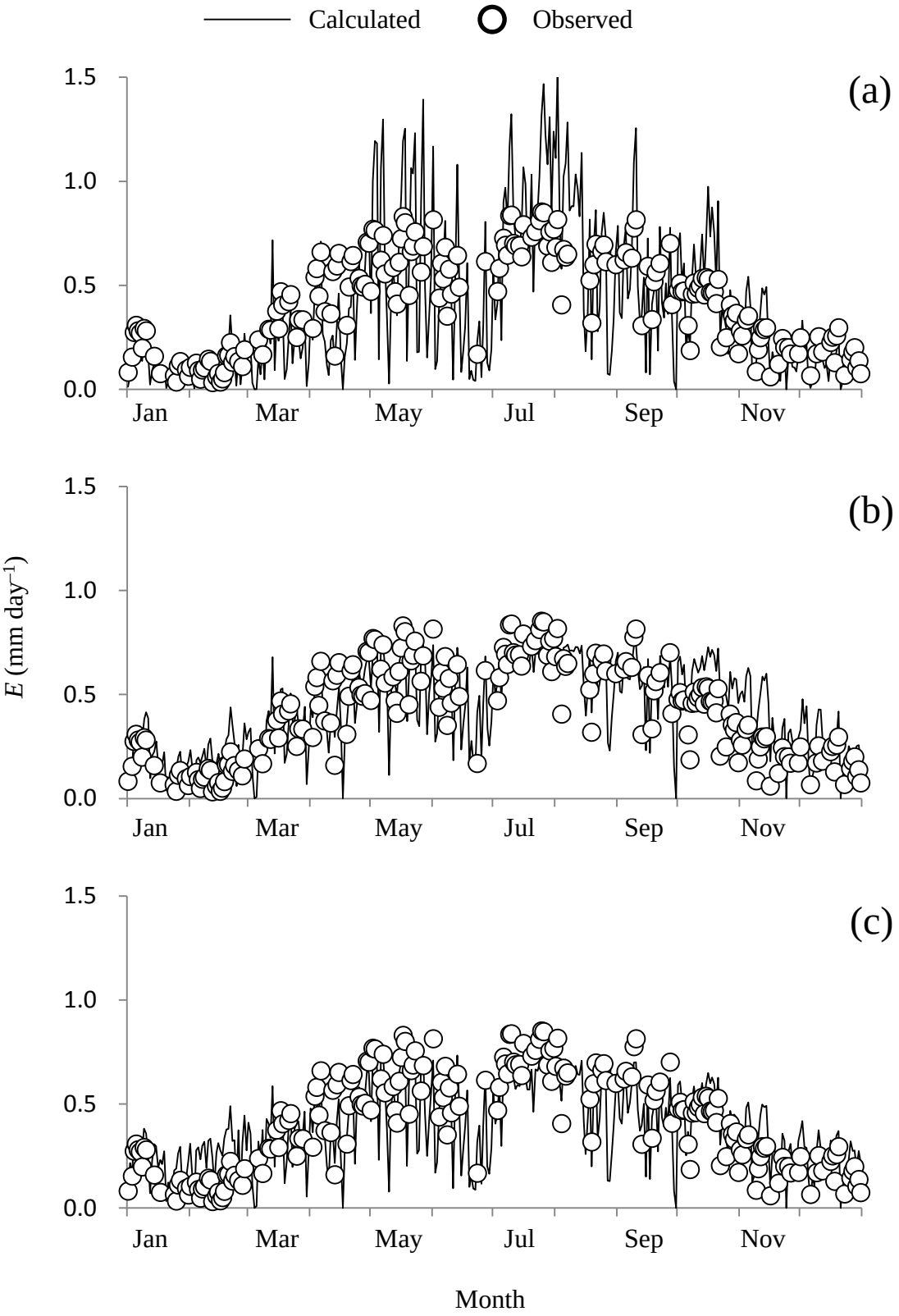

Figure 9

Table 1. Location, meteorology (the mean annual rainfall P and temperature T), structure (stem density N, the mean diameter at breast height d_m, leaf area index L, and sapwood area A), and description of sap-flux measurements for the plantation sites

Site [*1]	Location	P (mm)	T (°C)	Age (yr)	N (stems ha^{-1})	d_m (cm)	L (m^2 m^{-2})[*2]	A (m^2 ha^{-1})	Plot area (m^2)	Number of the trees in the plot	Period	Reference
Cedar												
IK	36°N, 137°E	2814	12.7	55	600	48.4	3.2	36.6	300	18 (9) [*3]	May 15, 2010–May 24, 2011	Shinohara et al. (2013a)
YB	34°N, 131°E	1790	17.2	39	1100	28.9	4.7	22.4	100	11 (11)	Aug 1–Sept 31, 2010	Komatsu et al. (2013)
YA	34°N, 131°E	1790	17.2	40	600	31.6	2.3	14.1	100	6 (6)	Aug 1–Sept 31, 2011	Komatsu et al. (2013)
IS	34°N, 131°E	1807	15.9	43	658	28.2	0.8	21.5	213	14 (11)	May 22, 2012–Feb 28, 2013	Xiang et al. (submitted)
IR	34°N, 131°E	1790	17.2	60	1400	30.3	3.3	28.4	200	28 (14)	July 1–Aug 31, 2010	Ichihashi et al. (in press)
KL	33°N, 131°E	2150	15.0	50	904	40.3	5.7	46.0	321	29 (15)	Mar 3, 2007–July 3, 2008	Kumagai et al. (2007)
KU	33°N, 131°E	2150	15.0	50	1575	23.8	5.4	36.3	318	50 (23)	Mar 3, 2007–July 3, 2008	Kumagai et al. (2007)
KS	33°N, 131°E	2150	15.0	50	1330	26.6	5.9	37.3	203	27 (19)	Mar 3, 2007–July 3, 2008	Kumagai et al. (2014)
XT	24°N, 121°E	2635	17.0	60	625	39.0	2.6	18.4	400	25 (15)	Apr 14, 2012–Mar 19, 2013	Laplace (2013)
Cypress												
IH	34°N, 131°E	1807	15.9	43	863	20.2	0.8	8.8	197	17 (17)	May 22, 2012–Feb 28, 2013	Xiang et al. (submitted)
OL	34°N, 131°E	1790	17.2	49	1450	21.0	3.2	20.4	400	58 (14)	Jan 1–Dec 31, 2008	Kume et al. (2010)
OU	34°N, 131°E	1790	17.2	49	1700	14.9		16.8	100	58 (17)	Jan 1–Dec 31, 2008	Kume et al. (submitted)
SK	34°N, 131°E	1790	17.2	19	2100	13.5	4.8	20.4	100	21 (10)	Apr 1–Aug 15, 2009	Tsuruta et al. (submitted)
HW	34°N, 131°E	1790	17.2	99	350	44.6	3.1	15.2	200	7 (7)	Apr 1–Aug 31, 2009	Tsuruta et al. (submitted)

[*1] The original names of the sites are given as follows. IK: Ishikawa-ken Forest Experimental Station, YB: Yamanokami site (before thinning), YA: Yamanokami site (after thinning), IS: Yayama Experimental Catchment (cedar) in Iizuka, IR: Ichirinpan Plot in the Kasuya Research Forest, KU: UP of Kahoku Experimental Watershed, KL: LP of Kahoku Experimental Watershed, KS: SP of Kahoku Experimental Watershed, XT: Xitou Experimental Forest, IH: Yayama Experimental Catchment (cypress) in Iizuka, OL: Riparian Plot of Ochozu Experimental Watershed, OU: Ridge Plot of Ochozu Experimental Watershed, SK: Sakuta Plot in Kasuya Research Forest, HW: Hiawada Plot in Kasuya Research Forest

[*2] L for all sites except OL and IK was measured using a plant-canopy analyzer (LAI-2000, Li-Cor Inc., Lincoln, Nebraska, USA). L for OL and IK was measured using a digital non-spherical color photograph and Gap Light Analyzer software (Franzer et al., 1999).

[*3] Numerals in the parentheses indicate the number of trees in which sensors were installed.

Table 2. Parameter values optimized for each site .

Site	G_{cref} (mm s^{-1})	β in $f(D)$	R^2	δ in $g(R)$	R^2	ε (°C) in $h(T)$	ζ (°C) in $h(T)$	R^2
Cedar								
IK	9.77	0.750	0.782	0.287	0.389	7.75	0.313	0.469
YB	3.46	0.441	0.493	0.0893[*1]	0.00793			
YA	1.89	0.427	0.365	0.0625[*1]	0.00247			
IS	2.84	0.569	0.580	0.238	0.339	20.7	–48.8	0.164
IR	2.81	0.351	0.214	0.288	0.219			
KL	6.07	0.783	0.605	0.347	0.316	12.3	0.065	0.587
KU	4.22	0.749	0.438	0.410	0.240	15.1	–5.22	0.343
KS	5.19	0.667	0.628	0.378	0.392	14.8	–2.49	0.544
XT	2.84	0.412	0.213	0.308	0.310			
Cypress								
IH	1.76	0.472	0.622	0.000[*1]	–0.0329	21.0	–2.84	0.740
OL	3.22	0.453	0.628	0.285	0.330	18.2	–5.19	0.636
OU	1.86	0.591	0.738	0.417	0.561	17.2	–5.78	0.584
SK	5.65	0.468	0.412	0.432	0.252			
HW	2.81	0.688	0.436	0.441	0.270			
Mean	3.89	0.556		0.285		15.9	–8.74	
Standard deviation	2.19	0.146		0.142		4.43	16.4	

[*2] A small δ value does not suggest that there was no effect of solar radiation on transpiration, but suggests that the effect was not detectable by an analysis on a daily time scale.

Table 3. Slope and coefficient of determination (R^2) for the relationship between calculated and observed transpiration.

Site	P1W		P2W		P3W	
	Slope [*1]	R^2	Slope	R^2 [*2]	Slope	R^2
Cedar						
IK	2.43	0.329 [*3]	0.946	0.329	1.02	0.576
IS	0.776	0.867	1.06	0.867	1.03	0.874
KL	1.50	0.845	0.964	0.845	1.04	0.818
KU	1.05	0.757	0.970	0.757	1.06	0.726
KS	1.32	0.848	0.988	0.848	1.05	0.845
Cypress						
IH	0.510	0.927	1.13	0.927	1.02	0.937
OL	0.879	0.843	1.06	0.843	1.04	0.883
OU	0.466	0.891	0.974	0.891	1.05	0.911

[*1] The intercept of the regression equation was assumed to be zero.

[*2] Determination coefficients for P2W are identical to those for P1W, because the responses of canopy conductance to meteorological factors for P2W are same as those for P1W.

[*3] Low determination coefficients for IK were primarily caused by the small number of data with low E due to rejection of data recorded on rainy days. When including data recorded on rainy days in the analysis, the determination coefficients were 0.829, 0.829, and 0.858 for P1W, P2W, and P3W, respectively.